Land Area Change and Fractional Water Maps in the Chenier Plain, Louisiana, Following Hurricane Rita (2005)

By Monica Palaseanu-Lovejoy, Christine Kranenburg, and John C. Brock

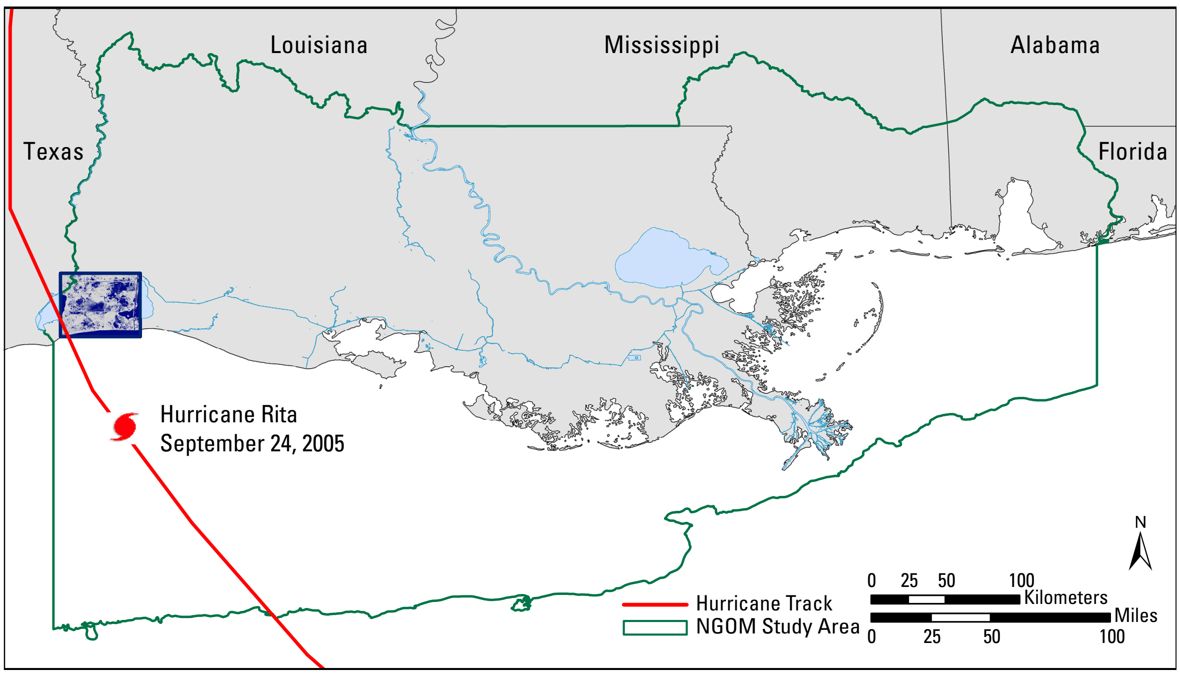

Pamphlet to accompany

Scientific Investigations Map 3141

U.S. Department of Interior
U.S. Geological Survey

U.S. Department of the Interior
KEN SALAZAR, Secretary

U.S. Geological Survey
Marcia K. McNutt, Director

U.S. Geological Survey, Reston, Virginia: 2010

For product and ordering information:
World Wide Web: http://www.usgs.gov/pubprod
Telephone: 1-888-ASK-USGS

For more information on the USGS—the Federal source for science about the Earth, its natural and living resources, natural hazards, and the environment:
World Wide Web: http://www.usgs.gov
Telephone: 1-888-ASK-USGS

Suggested citation:
Palaseanu-Lovejoy, M.E., Kranenburg, C.J., Brock, J.C., 2010, Land area change and fractional water maps in the Chenier Plain, Louisiana, following Hurricane Rita, (2005): U.S. Geological Survey, Scientific Investigations Map 3141, 6p. pamphlet.

Contents

Introduction 1
Methodology 1
Discussion 2
Conclusion 5
Acknowledgments 6
References 6

Figures

Figure 1. Example of fractional water map (2003 data), the Chenier Plain, Louisiana 2
Figure 2. Methodology flowchart for creation of fractional water map. 3
Figure 3. Change analysis map, the Chenier Plain, Louisiana 5

Tables

Table 1. Independent and dependent variable predictors. 4
Table 2. Evaluation indices for maximum Kappa coefficient of agreement (PCC, percent correctly classified; AUC, area under the curve). 4
Table 3. Percent correctly classified (PCC) results for selection and validation points, and comparison with similar land/water classification maps for post-Hurricane Rita image 4

U.S. Geological Survey — science for a changing world

Scientific Investigations Map 3141
Pamphlet accompanies map

Land Area Change and Fractional Water Maps in the Chenier Plain, Louisiana, following Hurricane Rita (2005)

By Monica Palaseanu-Lovejoy,[1] Christine Kranenburg,[1] and John C. Brock[2]
[1]Jacobs Technology, contracted to U.S. Geological Survey, St. Petersburg, FL, [2]U.S. Geological Survey, Reston, VA

2003

Fractional Water

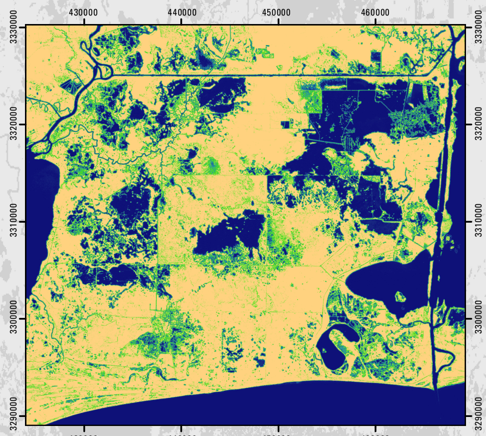

Land/Water Classification
Maximum Kappa Threshold

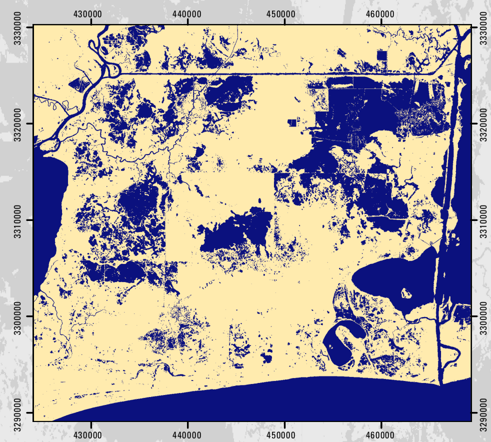

Percent Water: 100 – 0

0 5 10 Kilometers

Threshold	PCC	PCC Water	PCC Land	Kappa	AUC	Commission	Omission
51%	99.13%	98.73%	99.52%	98.26%	99.92%	0.52%	1.27%

Percentage Correctly Classified (PCC)
Area Under the Curve (AUC)

Explanation
Land
Water

2006

Fractional Water

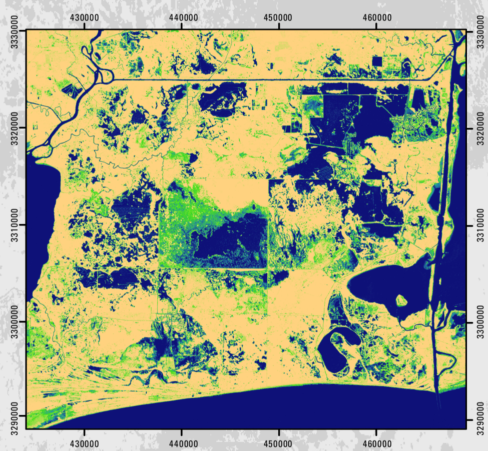

Land/Water Classification
Maximum Kappa Threshold

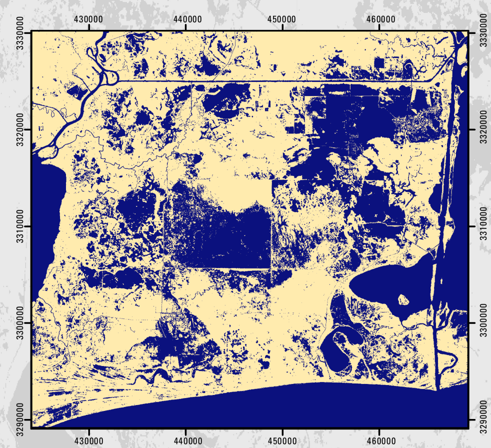

0 5 10 Kilometers

Threshold	PCC	PCC Water	PCC Land	Kappa	AUC	Commission	Omission
26%	98.96%	98.42%	99.52%	97.92%	99.92%	0.47%	1.58%

Percentage Correctly Classified (PCC)
Area Under the Curve (AUC)

Projected using the WGS 84 datum and the UTM Zone 15N coordinate system.

Image Sources:
Landsat 7 Enhanced Thematic Mapper Plus (ETM+) satellite imagery acquired on April 17, 2003, and Landsat 5 Thematic Mapper (TM) imagery acquired on February 12, 2006.
IKONOS and QuickBird high resolution imagery acquired on May 23, 2003, and March 25, 2006, respectively.
All imagery provided by USGS Earth Resources Observation and Science (EROS) Center.
(The data are projected using the WGS 84 datum and the UTM Zone 15N coordinate system.)

Suggested citation:
Palaseanu-Lovejoy, M.E., Kranenburg, C.J., and Brock, J.C., 2010, Land area change and fractional water maps in the Chenier Plain, Louisiana, following Hurricane Rita (2005): U.S. Geological Survey Scientific Investigations Map 3141, 1 sheet, 6 p. pamphlet.

See pamphlet for references cited.

Land Area Change Following Hurricane Rita (2005)

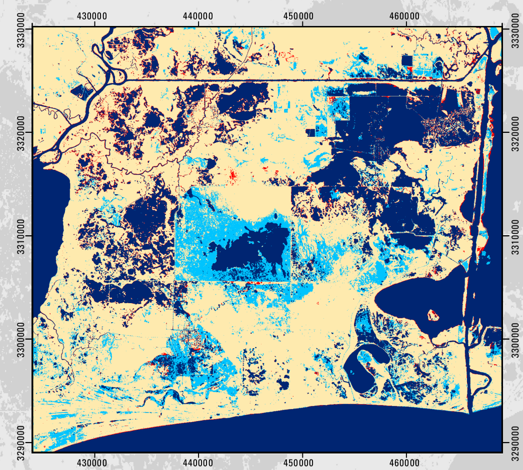

0 5 10 Kilometers

- New Water Areas (9.4%)
- New Land Areas (2.6%)
- Unchanged Land Areas (54.3%)
- Unchanged Water Areas (33.7%)

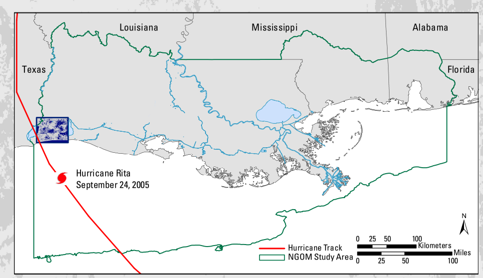

Northern Gulf of Mexico (NGOM) study area showing the track of Hurricane Rita in relation to the land change study area of this map.

U.S. Department of the Interior
U.S. Geological Survey

December 2010

Land Area Change and Fractional Water Maps in the Chenier Plain, Louisiana, following Hurricane Rita (2005)

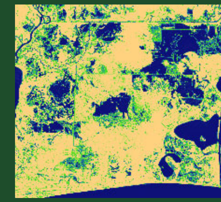

By Monica Palaseanu-Lovejoy, Christine Kranenburg, and John C. Brock

Introduction

In this study, we estimated the changes in land and water coverage of a 1,961-square-kilometer (km²) area in Louisiana's Chenier Plain. The study area is roughly centered on the Sabine National Wildlife Refuge, which was impacted by Hurricane Rita on September 24, 2005. The objective of this study is twofold: (1) to provide pre- and post-Hurricane Rita moderate-resolution (30-meter (m)) fractional water maps based upon multiple source images, and (2) to quantify land and water coverage changes due to Hurricane Rita.

Methodology

The USGS Earth Resources Observation and Science (EROS) Center provided the following imagery for this project: a Landsat 7 Enhanced Thematic Mapper Plus (ETM+) satellite image acquired for Path 24, Row 39, on April 17, 2003, a Landsat 5 Thematic Mapper (TM) image acquired on February 12, 2006, and one each of a QuickBird and IKONOS high-resolution image acquired on May 23, 2003, and March 25, 2006, respectively.

A series of vegetation and water indices (Horne, 2003; Zha and others, 2003; Wales, 2005; Yarbrough and others, 2005; Navulur, 2006; Xu, 2006; Jenson, 2007) and transforms was created using the high-resolution imagery at a 4-m scale and thresholded to obtain a binary land/water map. Using a method developed in Yang and others (2003a,b), a 30-m grid was overlaid on the binary map, and the water pixels in each grid cell were counted to generate a water percentage map at 30 m, henceforth referred to as the dependent variable. The areal extent of this percent water map corresponds to the extent of the high-resolution image. Using the National Land Cover Data (NLCD) Mapping Tool module for ERDAS IMAGINE (ERDAS, 2006), 100,000 stratified random sample points with a minimum of 1,000 points per stratum were selected from the dependent variable as training points for the independent variable layers. The independent variables consist of the six thematic bands of the Landsat imagery, Haralick texture (Haralick and others, 1973) features for each Landsat band (second moment, correlation, contrast, dissimilarity, entropy, homogeneity, mean, and variance), principal components (PCA), independent components (ICA), tasseled cap transformation (TCT) components, and an expanded set of water and vegetation indices derived from the Landsat image. More specialized water indices are possible at the Landsat scale because of the added availability of the two mid-IR bands, which are not present in the QuickBird/ and IKONOS imagery.

Correlations between all independent variables were computed in order to minimize colinearity and overfitting. The rules for the regression tree were created for each combination of independent and dependent variables using the data-mining software RuleQuest Cubist v. 2.05 (RuleQuest Research, 2010). The resulting regression model was applied to the independent variables to obtain a fractional water map (fig. 1) whose aerial extent covers the entire study area. The methodology flowchart is presented in figure 2.

To determine the best result from the more than 400 parameter combinations run, over 6,000 random points were generated and unambiguously classified using corresponding aerial photographs. These map selection points and the percent water maps were analyzed by an R-language optimization procedure (Atkinson and Mahoney, 2004; Wirtschaftsuniversität Wien, 2009) to determine the threshold at which the maximum Kappa coefficient occurs. The procedure calculates the confusion matrix, percentage correctly classified (PCC), Kappa coefficient of agreement, receiver operating curve (ROC), area under the curve (AUC), and p-values of differences in AUC between models for the optimized Kappa threshold and a fixed threshold of 0.5. The list of independent and dependent variables that were useful predictors and the results of the accuracy assessment for the final maps selected for 2003 and 2006 are shown in table 1 and table 2.

An accuracy assessment was done using 1,000 random points also classified using corresponding aerial photographs but separate from the points used for map selection. Whereas ambiguous (in terms of photo-interpretation) points were eliminated from the selection dataset, no restrictions were placed on the accuracy assessment points. For the post-Rita image (2006), we also had a classified land/water map developed by J. Barras, USGS (oral commun., 2009) and the National Oceanic and Atmospheric Administration (NOAA) Coastal Change Analysis Program (C-CAP) map (NOAA, 2006), which was re-coded into a binary land/water map. The results of the comparison are presented in table 3.

Quantification of the percent land change from pre- to post-Rita land/water classification maps was done

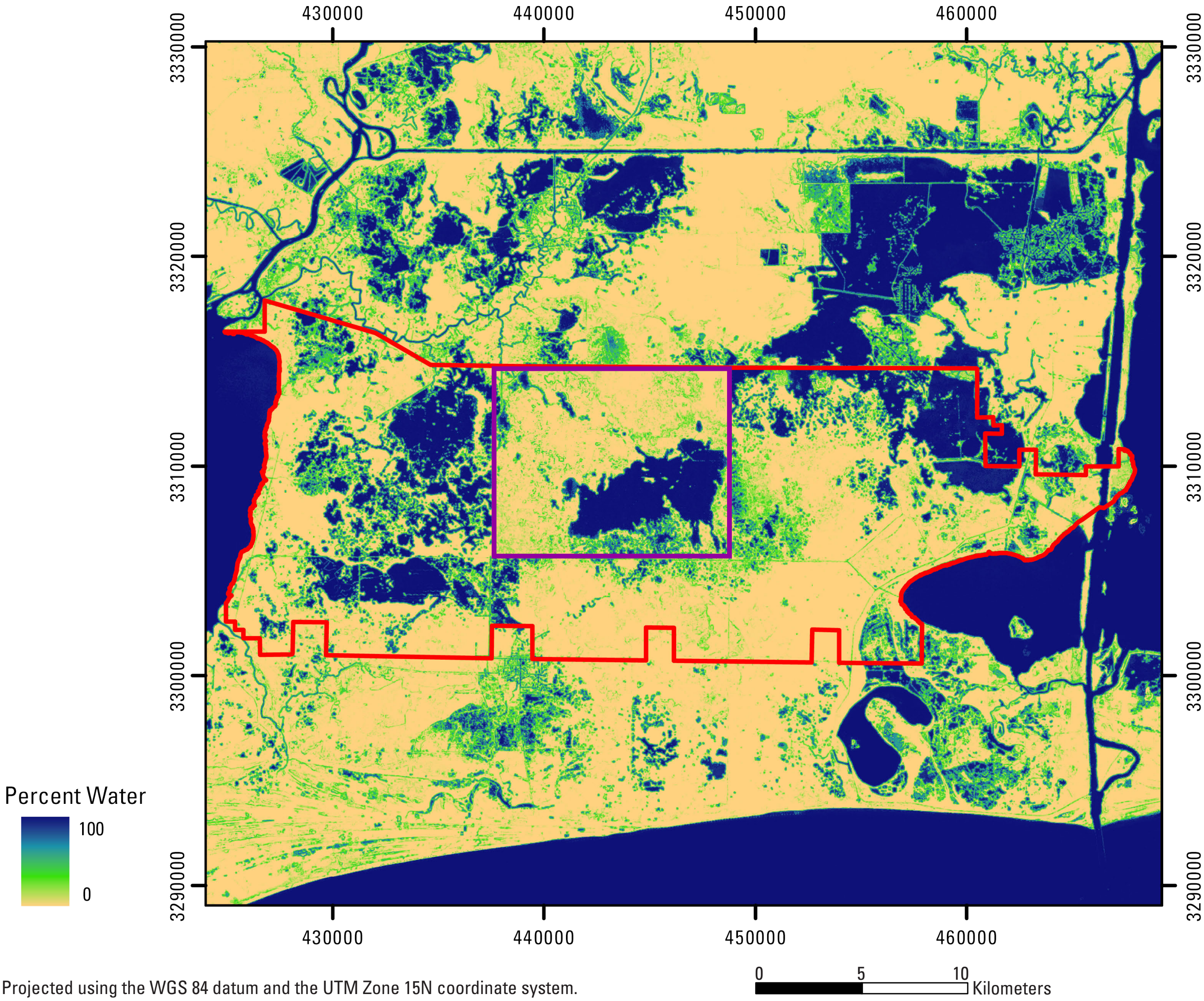

Figure 1. Example of fractional water map (2003 data), the Chenier Plain, Louisiana. Sabine National Wildlife refuge is highlighted in red. The Five Lakes area is highlighted in violet.

by subtracting one classification from the other. The accompanying change map (fig. 3) highlights all gains and losses that occurred during the comparison interval. It does not take into consideration differences in water levels (tidal or meteorological). The water levels were checked for imagery acquisition dates and times at six distinct water stations in the area, and the maximum difference in water levels does not exceed 15 centimeters (cm).

Discussion

The 2003 Landsat ETM+ image used for pre-Rita conditions can be considered a good baseline since in the previous 25 years only two low-intensity tropical storms made landfall within the study area, and all the major hurricanes in the vicinity (intensity greater or equal to 3 on the Saffir-Simpson scale) were 100 km or more from the study area (NOAA, 2008).

The Chenier Plain is a very complex area because it contains multiple, heterogeneous impoundments that encompass wetlands, pasture and cultivated fields, as well as industrial and residential areas. These areas can trap water for long periods of time, and drainage is often controlled by artificial means, contributing to the challenging interpretation of the land/water features and their persistence. Each of these distinct land-use types responds to and recovers differently from an extreme storm event. Thus, land/water changes detected after an extreme storm event reflect both permanent and temporary changes. Permanent new water areas are the result of direct removal of wetlands by storm surge and appear mostly connected to existing bodies of open water, or emerge in marsh fringing areas. However, new water areas unconnected

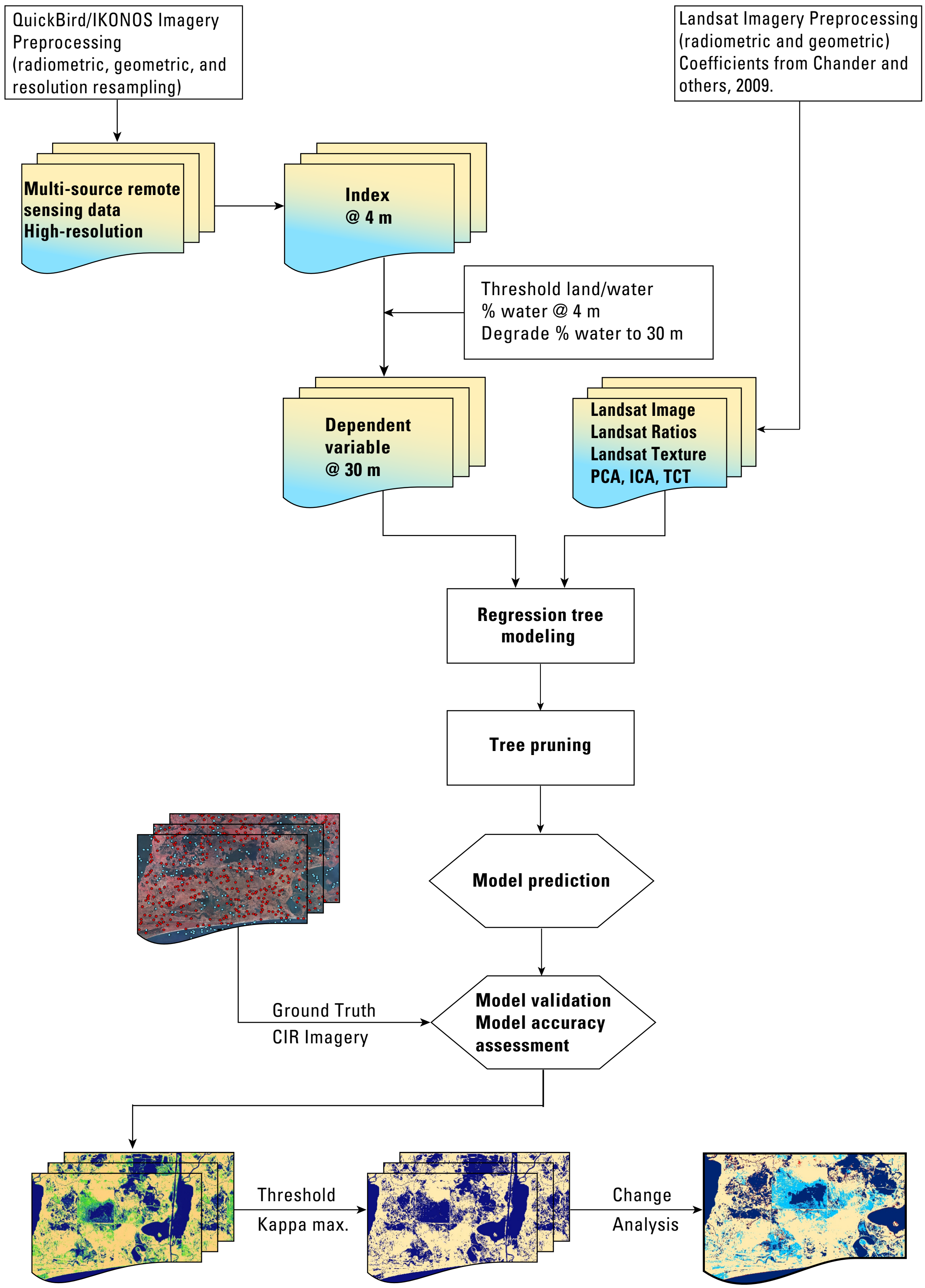

Figure 2. Methodology flowchart for creation of fractional water map. Principal Component Analysis (PCA), Independent Component Analysis (ICA), Tasseled Cap Transformation (TCT).

Table 1. Independent and dependent variable predictors.

Year	Independent variables	Dependent variable
2003	Landsat bands: 1 to 6	Water Index: b1/b4
	Texture: Variance bands 1 to 6	
	Water Index: (sum(vis)-sum (IR))/(sum(vis)+sum(IR))	
2006	Landsat bands: 1 to 6	Water Index: TCT1or2 = Logical OR combination of tasseled cap transform bands 1 and 2.
	Texture: Homogeneity bands 1 to 6	
	Independent Components (3): bands 1 to 3	

Table 2. Evaluation indices for maximum Kappa coefficient of agreement (PCC, percent correctly classified; AUC, area under the curve).

Year	Threshold	PCC	PCC Water	PCC Land	Kappa	AUC	Commission	Omission
2003	51%	99.13%	98.73%	99.52%	98.26%	99.92%	0.52%	1.27%
2006	26%	98.96%	98.42%	99.52%	97.92%	99.92%	0.47%	1.58%

to previous water bodies are also observed in historically dry, stable areas such as south of the Sabine National Wildlife Refuge, which is highlighted in red on figure 1 (Barras, 2009).

Temporary new water bodies are usually the result of flooding and water entrapment in impounded areas, removal or scouring of floating and submerged vegetation, or are caused by water-level fluctuation due to tidal and (or) meteorological variations between images. A particularly difficult section to interpret is the Five Lakes area impoundment (highlighted in violet on fig. 1), in the center of the Chenier Plain study area. Discussions with local area managers revealed that this area is a freshwater marsh that was flooded by saltwater during Hurricane Rita. Compounding the problem, large mats of marsh wrack deposited by the hurricane into the canal on the southern edge of the impoundment prevented it from draining. As a consequence, the vegetation suffered severe salt burn and prolonged inundation. It represents about 2.16 percent of the total study area. It is clear that the marsh did not recover by February 2006. What is not clear is how much water actually drained from the impoundment. As previously mentioned, making a clear distinction between permanent and temporary changes to water bodies is a complicated task, which becomes even more difficult after a major storm event. Caution is needed in correctly assessing this area for any further interpretation.

Land gain in the Chenier Plain is mostly transitory and is the effect of storm-debris deposition, displacement of aquatic vegetation to different locations, and water-level fluctuations. The majority of the land gain seen along rivers, canals, and beaches is a direct result of variations in water levels due to tidal or meteorological influences. About 1 percent of the image area is affected in at least one of the inputs by clouds, cloud shadows, and contrails. Although they are not currently

Table 3. Percent correctly classified (PCC) results for selection and validation points, and comparison with similar land/water classification maps for post-Hurricane Rita image.

2003	Selection: PCC (6804 points)				Validation: PCC (1000 points)		
		Land	Water	Total	Land	Water	Total
		99.52%	98.73%	99.13%	96.37%	89.07%	93.70%
2006	**Selection: PCC (6344 points)**				**Validation: PCC (1000 points)**		
	Model	**Land**	**Water**	**Total**	**Land**	**Water**	**Total**
	USGS	99.52%	98.42%	98.96%	91.35%	91.99%	91.60%
	J. Barras (USGS, 2009)	99.94%	86.76%	93.24%	95.60%	76.74%	88.30%
	C-CAP (NOAA)	99.87%	79.00%	89.27%	97.23%	72.87%	87.80%

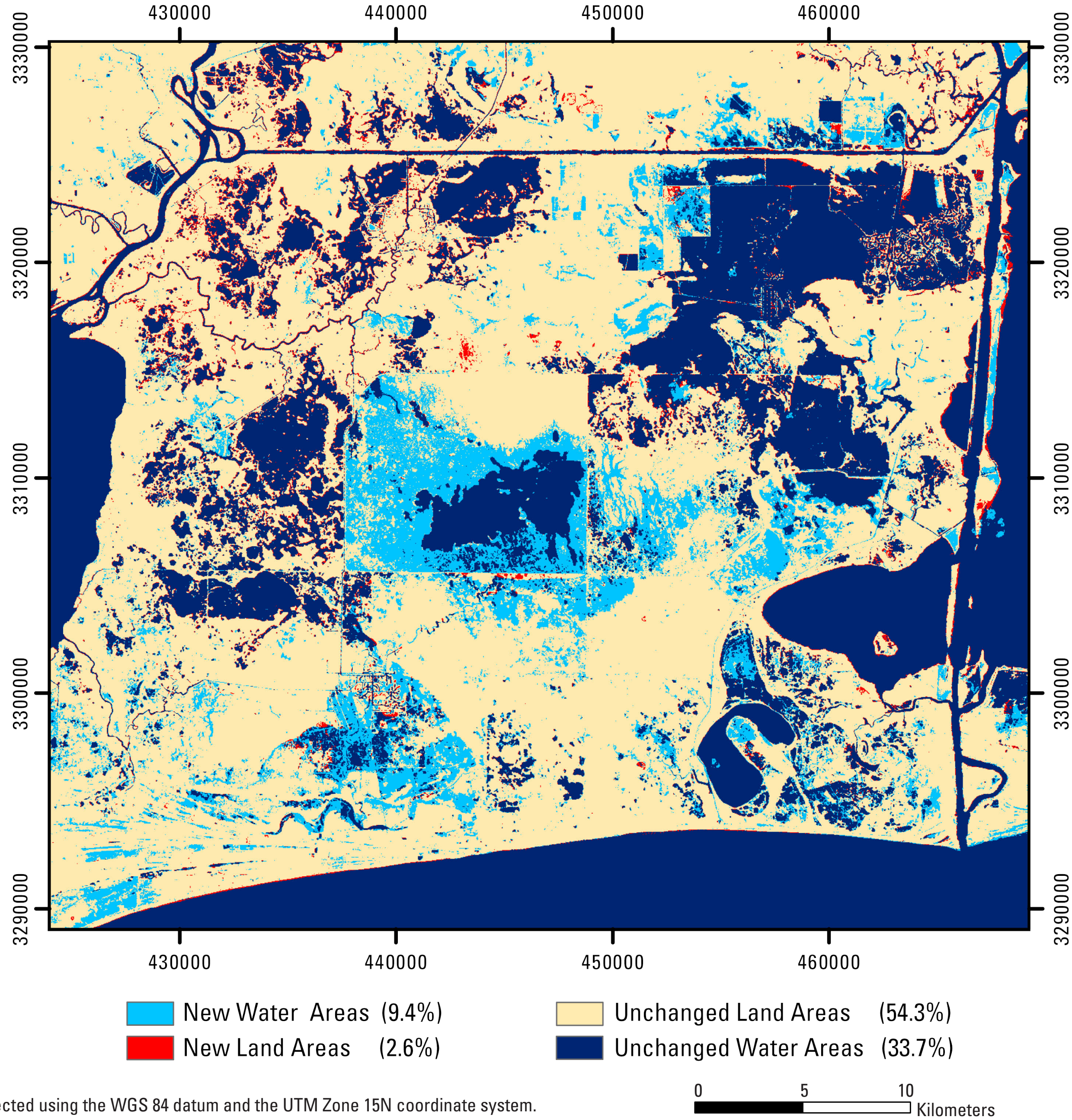

Figure 3. Change analysis map, the Chenier Plain, Louisiana.

masked out in the results, they are clearly not to be relied upon. A mask image is provided with the dataset.

Conclusion

The increase in water area of about 10 percent between 2003 and 2006 is attributed to both permanent and temporary changes in land/water configuration. The majority of new water areas occurs around previous bodies of open-water and in marsh fringing areas, but they are also present in historically stable areas. The presence of scarring in stable marshes is associated with preexisting open water ponds, but in some areas it is difficult to discriminate between flooded marshes or marshes removed by storm surge. Storm-debris deposition can result in small new land areas, but land gain along waterways and beaches is considered the result of temporary variations in water levels due to tidal or meteorological influences.

Estimation of permanent losses (or gains) cannot be made until the transitory impacts are identified and quantified. However, it is expected that the permanent losses will be significant since the area did not have enough time to recover before the next extreme storm event, which occurred on

September 13, 2008, when Hurricane Ike made landfall as a Category 2 storm.

Acknowledgments

The USGS St. Petersburg Coastal and Marine Science Center acknowledges the support and assistance of the USGS Land Characterization team at the Earth Resources Observation and Science (EROS) Center, in Sioux Falls, S. Dak., and the USGS National Wetlands Research Center, in Baton Rouge, La., in the development of this dataset.

References

Atkinson, E.J. and Mahoney, D.W., 2004, Mayo Foundation for Medical Education and Research: S-Plus/R functions database, accessed online July 2008, at http://mayoresearch.mayo.edu/mayo/research/biostat/splusfunctions.cfm.

Barras, J.A., 2009, Land area change and overview of major hurricane impacts in coastal Louisiana, 2004-08: U.S. Geological Survey Scientific Investigations Map 3080, scale 1:250,000, 6 p. pamphlet. (Also available at: http://pubs.usgs.gov/sim/3080.)

Chander, G.D., Markham, B.L., and Helder, D.L., 2009, Summary of current radiometric calibration coefficients for Landsat MSS, TM, ETM+, and EO-1 ALI sensors: Remote Sensing of Environment, v. 113, p. 893-903.

ERDAS IMAGINE 9.1, 2006, Atlanta GA, ERDAS Inc.

Haralick, R.M., Shanmugam, K.S., and Dinstein, I.H., 1973, Textural features for image classification: IEEE Transactions on Systems, Man and Cybernetics, v. 3, no. 6, p. 610-621.

Horne, J.H., 2003, A tasseled cap transformation for IKONOS images–Proceedings of the American Society of Photogrammetry and Remote Sensing, 2003: Anchorage, Alaska, one CD-ROM.

Jenson, J.R., 2007, Remote sensing of the environment: An Earth resource perspective (2d ed.): Upper Saddle River, N.J., Prentice Hall, 544 p.

National Oceanic and Atmospheric Administration (NOAA), Coastal Services Center, 2006, C-CAP US (United States) Gulf Coast Zone 37/46 Area Post-Hurricane Katrina Land Cover Project, (also available at: http://www.csc.noaa.gov/crs/lca/katrina/).

National Oceanic and Atmospheric Administration (NOAA), Coastal Services Center, 2008, Historical North Atlantic Tropical Cyclone Tracks, 1851-2007, (also available at: http://csc-s-maps-q.csc.noaa.gov/hurricanes/viewer.html).

Navulur, K.C.S., 2006, Multispectral image analysis using the object-oriented paradigm: Remote Sensing Applications Series, Boca Raton, Fla., CRC Press, 184 p.

RuleQuest Research, 2010, Cubist v. 2.05: St. Ives, NSW 2075, Australia, (also available at: http://www.rulequest.com),

Wales, P.M., 2005, Quantitative analysis of land loss in coastal Louisiana using remote sensing: Oxford, University of Mississippi, Master's thesis, 91 p.

Wirtschaftsuniversität Wien, 2009 [Department of Statistics and Mathematics], The comprehensive R archive network database, accessed July 2009 at http://cran.r-project.org/.

Xu, Hanqiu, 2006, Modification of normalised difference water index (NDWI) to enhance open water features in remotely sensed imagery: International Journal of Remote Sensing, v. 27, no. 14, p. 3025-3033.

Yang, Limin, Huang, Chengquan, Homer, C.G., Wylie, B.K., and Coan, M.J., 2003a, An approach for mapping large-area impervious surfaces: Synergistic use of Landsat-7 ETM+ and high spatial resolution imagery: Canadian Journal of Remote Sensing, v. 29, no. 2, p. 230-240.

Yang, Limin, Xian, George., Klaver, J.M., and Deal, Brian, 2003b, Urban land-cover change detection through sub-pixel imperviousness mapping using remotely sensed data: Photogrammetric Engineering and Remote Sensing, v. 69, no. 9, p. 1003-1010.

Yarbrough, L.D., Easson, G.L., and Kuszmaul, J.S., 2005, QuickBird 2 tasseled cap transform coefficients: A comparison of derivation methods–Proceedings of the American Society of Photogrammetry and Remote Sensing, 2005: Sioux Falls, S. Dak., one CD-ROM.

Zha, Yong, Gao, Jay, and Ni, Shaoxiang, 2003, Use of normalized difference built-up index in automatically mapping urban areas from TM imagery: International Journal of Remote Sensing, v. 24, no. 3, p. 583-594.